A Reliability Comparison of Classical and Stochastic Thickness Margin Approaches to Address Material Property Uncertainties for the Orion Heat Shield

Steven A. Sepka [1]
AMA Corp., Moffett Field, CA 94043

Mary Kathleen McGuire[2] and Jeremy C. Vander Kam [3]
NASA Ames Research Center, Moffett Field, CA 94035

The Orion Thermal Protection System (TPS) margin process uses a root-sum-square approach with branches addressing trajectory, aerothermodynamics, and material response uncertainties in ablator thickness design. The material response branch applies a bondline temperature reduction between the Avcoat ablator and EA9394 adhesive by 60°C (108°F) from its peak allowed value of 260°C (500°F). This process is known as the Bond Line Temperature Material Margin (BTMM) and is intended to cover material property and performance uncertainties. The value of 60°C (108°F) is a constant, applied at any spacecraft body location and for any trajectory. By varying only material properties in a random (monte carlo) manner, the perl-based script mcCHAR is used to investigate the confidence interval provided by the BTMM. In particular, this study will look at various locations on the Orion heat shield forebody for a guided and an abort (ballistic) trajectory.

Nomenclature

BTMM	=	bond line temperature material margin
COV	=	coefficient of variation [SD/μ]
mBLT	=	maximum bond line temperature
μ	=	mean
SD	=	standard deviation
TPS	=	thermal protection system

I. Introduction

Ablator material response modeling of Orion's heatshield during Earth entry determines the necessary TPS thickness and mass needed for safe entry. There are several codes that are used for this purpose. Among them are: the Fully Implicit Ablation and Thermal Response[1] (FIAT) code, the Charring Material Thermal Response and Ablation Program[2] (CMA), the Charring Ablating Thermal Protection Implicit System Solver[3] (CHAR), the Standard Ablation Program[4] (STAB), the Two-Dimensional Implicit Thermal Response and Ablation Program for Charring Materials[5] (TITAN), and Three-Dimensional FIAT[6] (3dFIAT). The codes FIAT, TITAN, and 3dFIAT comprise a "suite" of 1D, 2D, and 3D solvers using the same implicit solver algorithms. CHAR is a 1D, 2D, and 3D solver. CMA and STAB are 1D solvers. These codes are used extensively to predict the amount of needed TPS material, surface recession, and in-depth temperatures.

---

[1]Sr. Research Scientist, AMA Corporation, Thermal Protection Materials and Systems Branch, NASA Ames Research Center, MS-234-1, Moffett Field, CA, 94035, Senior Member, AIAA.
[2]Aerospace Engineer, Systems Analysis Office, NASA Ames Research Center, MS 258-1 Moffett Field, CA 94035, Senior Member AIAA
[3]Aerospace Engineer, Systems Analysis Office, NASA Ames Research Center, MS 258-1 Moffett Field, CA 94035, Senior Member AIAA

Ablator thickness "margin" is the additional material in the design specification to account for uncertainties in aerodynamics, aerothermal environment, and material properties. A review of the margins process is given by Cozmuta et. al.[7] The current Orion approach is to use a Root-Sum-Square (RSS) methodology that has separate terms, or "branches," for thickness required to cover trajectory, aerothermodynamics, and material property uncertainties. For the materials branch, thickness is found by reducing the maximum allowable bond line temperature between the main TPS and its adhesive by 108°F (60°C). Sizing to a reduced bond line temperature limit in this RSS branch is a proxy method to margin against material property uncertainties. This process is called the Bondline Temperature Material Margin (BTMM). The value of 108°F (60°C) is inherited from past work and is applied to any vehicle body point and for any trajectory.

This study is to determine the confidence interval (1σ, 2σ, etc.) that the BTMM provides for material property uncertainties. To date, these values have not been determined, but strong interest exists in the Orion program to know if the 60°C BTMM is conservative or not, and by how much. In addition to determining the confidence intervals, it will be shown that values depend upon body point location and trajectory. This work will also determine which material properties, based on their amount of uncertainty, have the greatest influence on peak bond line temperatures and amount of recession. This information will direct the Orion program on where to focus their efforts to increase the confidence and safety of the heat shield.

A new, probabilistic, perl-based script called mcCHAR is used to find these confidence intervals. The underlying monte carlo approach of mcCHAR is the same as that used in mcFIAT.[8] Each of these codes can include aerodynamic, aerothermodynamics, and material uncertainties into one monte carlo application. A schematic diagram of the process used is given in Fig. 1. For this work, only the uncertainty in material properties is considered. The components of Guidance, Navigation, and Control (GNC) and aerothermodynamics are kept at their nominal values. Previous monte carlo work has included aerothermodynamic uncertainties.[9]

In the monte carlo loop shown in Fig. 1, the material properties are varied and then the CHAR input files are written. The CHAR "run" is then completed by use of parallel processing. The CHAR output values of interest here are maximum bond line temperature (mBLT) and recession. A representative value of each input variable is also recorded for correlation studies.

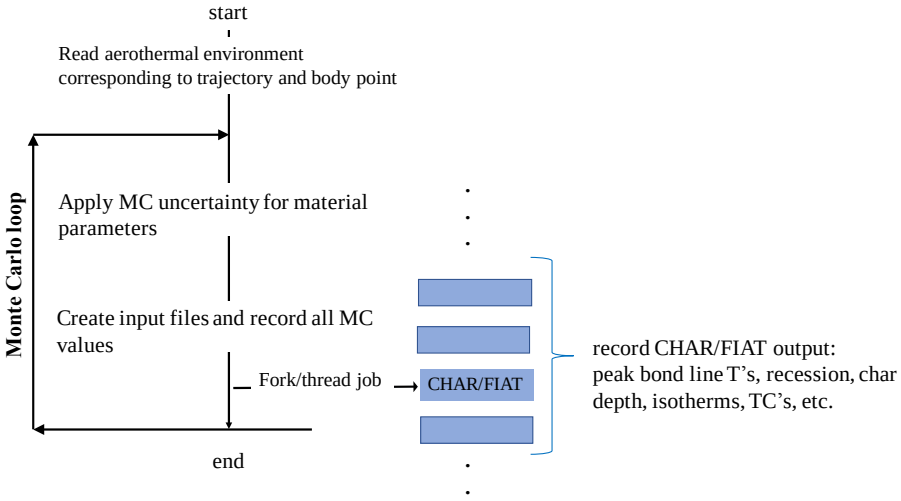

Figure 1. Schematic diagram of mcCHAR/mcFIAT operation for material property monte carlo

II. Monte Carlo Setup

Two trajectories are considered: one is a guided descent and the other is a ballistic/abort. These two trajectories are the driving cases for the current Orion TPS design thickness. Both of these trajectories are nominal with no flight mechanic uncertainties applied. Detailed information on these trajectories is given in the Appendix, see Table 5. At most body points, the guided trajectory will have lower heating rates (and lower recession) than the corresponding abort trajectory.

The material stackup consists of block Avcoat over 0.015 inches (0.000381 meters) of EA9394 adhesive and then the composite substructure material T300-EX1505. The thickness of T300-EX1505 varies based on body point location.

The EA9394 epoxy is an amine-cured epoxy paste adhesive with an aluminum powder filler.[10] It can be cured at room temperature and has excellent high temperature strength and toughness. The material also has excellent room temperature storability, good pot life, and excellent handling ability.[11]

For the composite material T300-EX1505, the designation T300[12] identifies the carbon fiber type and EX-1505[13,14] references a high service temperature, cyanate ester resin with high char yield.

A. Differences between Orion material properties and those used by mcCHAR

Nominal material properties used by mcCHAR are the same as those used in the Orion program with the exception of those given in Table 1. These updated values were found from additional information available to the program.

Table 1. Updated mcCHAR values

Virgin Density [kg/m^3]	599.891
EA9394 thickness [inch]	0.020
Initial temperature [K]	294.3

It is also noteworthy that the mcCHAR runs also include a manufacturing tolerance between 0 and 0.01 inches (0-0.000254 m) in a uniform random distribution of additional Avcoat thickness.

B. Body point locations

The seven body points for analysis in this study are shown as red circles in Fig. 2. Currently 321 body points are considered by the Orion program, and these are shown as blue circles. The numbering system is that the first coordinate, "I", represents the ray number. The second coordinate, "S", represents the position on the ray. A description of the seven analyzed body points is also given. These points are of interest to the Orion program.

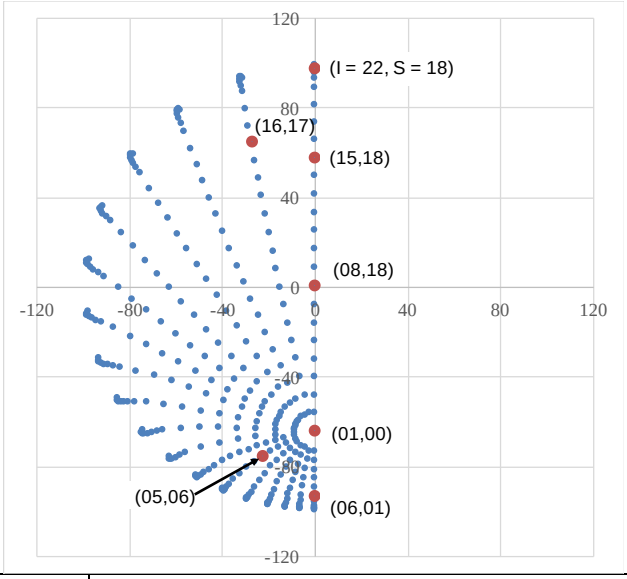

I01, S00	Stagnation point
I08, S18	Center of dish
I06, S01	Acreage at windward shoulder, centerline
I05, S06	Windside acreage, off-centerline
I15, S18	Leeward side, centerline, acreage
I16, S17	Leeward side, acreage, off-centerline
I22, S18	Leeward side, shoulder, centerline

Figure 2. Heat shield body point locations and their description.

C. Material property uncertainty values

The material uncertainty values are given in Table 2. A detailed explanation of the experimental techniques, data obtained, and data analysis are given in a separate paper.[15] The listed values, unless otherwise noted, are given as

twice the coefficient of variation (COV). This uncertainty represents a 95% confidence that a material property varies by +/- this amount.

These material properties are varied independently in the prescribed manner for each monte carlo run. If a correlation is known to exist between any two material properties, then the correlation is modeled and one of the variables is not considered in the analysis. For this study, pyrolysis gas enthalpy is scaled the same as char thermal conductivity and is not included in the analysis. It is thought that virgin density and char thermal conductivity may be correlated (i.e. Avcoat blocks with higher virgin density have higher thermal conductivity), but to date no correlation has been determined. It is the random nature of the monte carlo process that allows de-coupling of the material properties even though they may be related in a highly non-linear manner within CHAR.

The CHAR/FIAT predicted maximum bond line temperature and recession vary for each run. How material property values correlate to maximum bond line temperature and recession are important results of the monte carlo analysis. Thus it is critical to have a good estimate of uncertainty for every monte carlo parameter.

Table 2. List of CHAR variables available for McCHAR

All uncertainty distributions are Gaussian [2*COV] unless noted otherwise

mcCHAR Materal Parameter	**Uncertainty**
Initial temperature [K]	280.928-307.594 uniform
Initial surface pressure	0
Top TPS (Avcoat)	
Specific heat capacity, virgin	0.04
Specific heat capacity, char	0.04
Thermal conductivity, virgin	0.08
Thermal conductivity, char	0.18
Density, virgin [kg/m^3]	570.2573-629.5256 uniform
Density, char	0.07
Absortivity, virgin	0
Absortivity, char	0
Thickness, max additional [m]	0.00508 added
Permeability	0
Klinkenberg slip parameter	0
Porosity	0
Emissivity, virgin	0
Emissivity, char	0
Heat of formation, virgin	0
Heat of formation, char	0
Decomposition (each component)	
Pre-exponential factor	0.109 0.179 0.188
Reaction order	0.263 0.388 0.236
Activation temperature	0.060 0.061 0.033
B'tables	
B'c	0.15
Wall enthalpy	0.1
Density	0.04
Molecular weight	0.04
Roughness	
Roughness height	0.487
Height offset	-0.000223
Substructure	
Thickness, adhesive [m]	0.000254-0.000762 uniform
Thickness, composite [m]	+/-0.000127 uniform
Density	0.02
Specific heat capacity	0.02
Thermal conductivity	0.02

Note: pyrolysis gas enthalpy is scaled the same as char thermal conductivity and for correlation studies is not included in the analysis.

III. Procedure

First, one of the seven heat shield body point locations is selected along with a trajecory (guided or ballistic). The trajectory/body point combination is converted to an aerothermal environment. Then, the nominal Avcoat thickness is determined by CHAR. Finally, 10,000 CHAR runs (via mcCHAR) are completed using the nominal Avcoat thickness and varying only material properties.

The nominal Avcoat thickness is determined by sizing the Avcoat with the constraint that the bond line temperature between the Avcoat and EA9394 adhesive to not exceed 260°C (500°F). The material properties are all nominal.

For each monte carlo run, material property values, maximum bond line temperature, and amount of recession are recorded. Data analysis consists of: maximum bond line temperature (mBLT) and recession dispersions (histograms), gaussian statistics, correlation plots, and finding the confidence interval for each monte carlo run.

For all runs, the re-radiation temperature is 21.1°C (70°F). The re-radiation temperature is used for calculating the energy lost from the heat shield surface to the surrounding environment. The initial material temperature is 21.1°C.

IV. Presentation of Data and Discussion of Results

Of the seven body points analyzed, only one, the stagnation point, is presented here in detail. The results for the remaining body points are given in the appendix. For every mcCHAR analysis, there were 10,000 CHAR runs attempted and 10,000 solutions, giving a 100% converged solution success rate.

A. Stagnation point results

The location of the stagnation point on the heat shield is indicated by the red circle shown in Fig. 3. The coordinates of this body point are I=01, S=00. The results presented here are broken down into three subsections. The first, called "dispersions," analyzes how the CHAR predicted maximum bond line temperature (mBLT) and amount of recession varied over the 10,000 mcCHAR runs. The second subsection describes how the mBLT is correlated to the variation in material properties, and finally the third subsection describes how the amount of recession is correlated to the variation in material properties. These three subsections comprise the fundamental data analysis from the monte carlo run.

The mBLT for all runs is presented as a histogram with bin size of 5°C. These histograms are commonly referred to as dispersed sets or more simply as "dispersions."

For the correlation studies, a value of each material property is recorded for each monte carlo run. Correlation coefficient values are found for each material property with mBLT and amount of recession. A correlation coefficient value of 1.0 represents a perfect correlation between two variables. A negative value indicates an inverse relationship. Data are presented as pie charts of those material properties with the highest percentage of relative correlation, and tabulated data of the correlation values are given for these material properties. The pie charts were constructed by squaring the correlation coefficient of each variable.

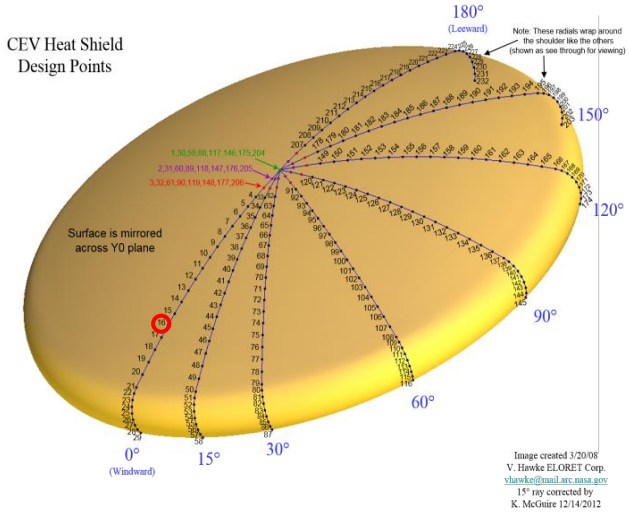

Figure 3. The location of stagnation point on heat shield is given by the red circle

1. Dispersions

The mBLT dispersions for the guided and abort/ballistic trajectories are shown in Fig. 4. The average mBLT is about 5° to 8°C below the prescribed 260°C maximum allowed bond line temperature (as shown as a red line in the figures). This difference is the result of the manufacturing tolerance that is used in mcCHAR. The standard deviation for the guided trajectory is ~19.1°C and for the ballistic trajectory is ~17.7°C. Both of these dispersions have a Gaussian shape.

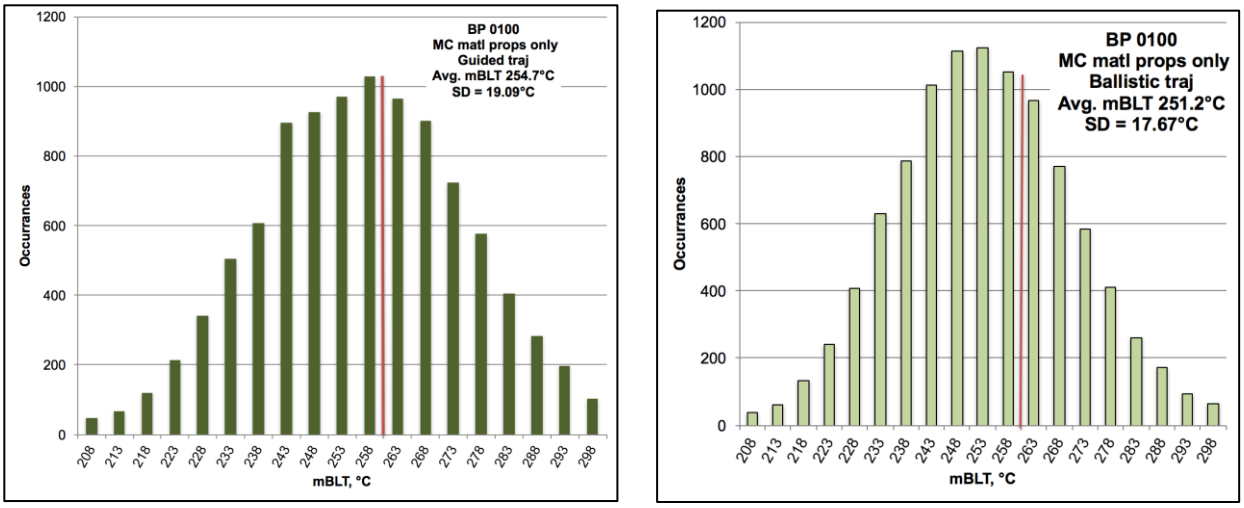

a) Guided trajectory b) Ballistic trajectory

Figure 4. Bond line temperature distributions at stagnation point

Shown in Fig. 5 are the recession dispersions for the guided and ballistic trajectories. The recession dispersion for the guided trajectory (Fig. 5a) is skewed, which is common when the amount of recession is very small. For this case, the average amount of recession is 0.035 in. (0.00089 m) with a standard deviation of 0.006 in. (0.00015 m). By visual inspection, the recession dispersion for the ballistic trajectory has a more Gaussian-like shape as shown in Fig. 5b. Here, the average recession is 0.104 in. (0.00264 m) with a standard deviation of 0.011 in. (0.00028 m).

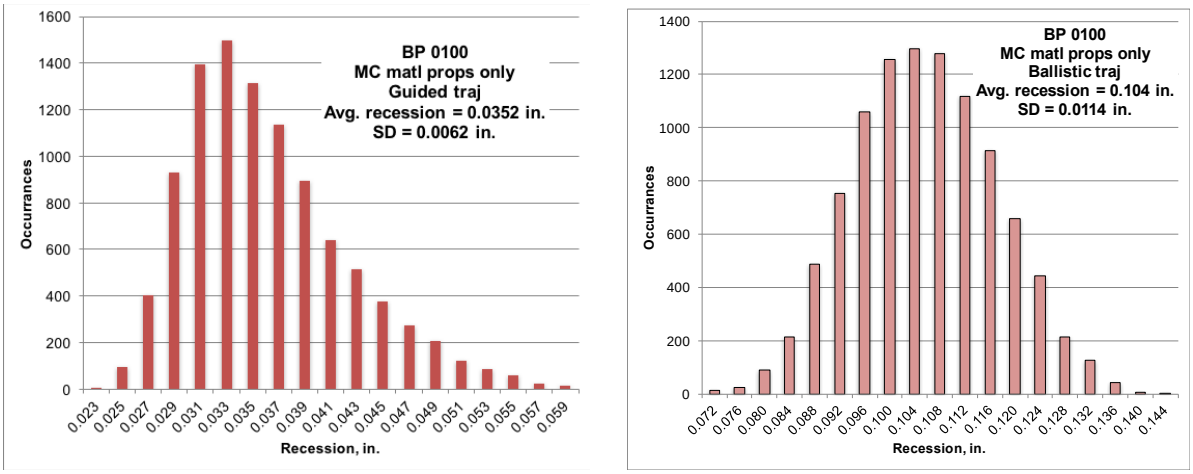

a) Guided trajectory b) Ballistic trajectory

Figure 5. Recession distributions at stagnation point

2. mBLT correlations

For the guided entry trajectory, the uncertainty in char thermal conductivity has the greatest relative correlation (70%) with mBLT, as shown in Fig. 6a, followed by virgin density (17%). Together these variables account for 87% of the relative influence on mBLT amongst all material properties. Char thermal conductivity has a correlation coefficient of 0.836, which indicates its very strong correlation on an absolute scale. The uncertainty in virgin thermal conductivity, initial TPS temperature, Avcoat thickness (there is a manufacturing tolerance) and char

density account for 2 to 4% relative importance each. All the remaining variables account for less than 1% combined.

The pie chart for the ballistic trajectory (see Fig. 6b) shows that uncertainty in char thermal conductivity (48%) has the most relative correlation on mBLT, followed by virgin density (28%), top TPS thickness (8%), initial TPS temperature (6%), char density (2%) and virgin thermal conductivity (3%). The sum of all other variables account for 5% of the relative sensitivity. Correlation coefficients range from 0.69 to 0.15.

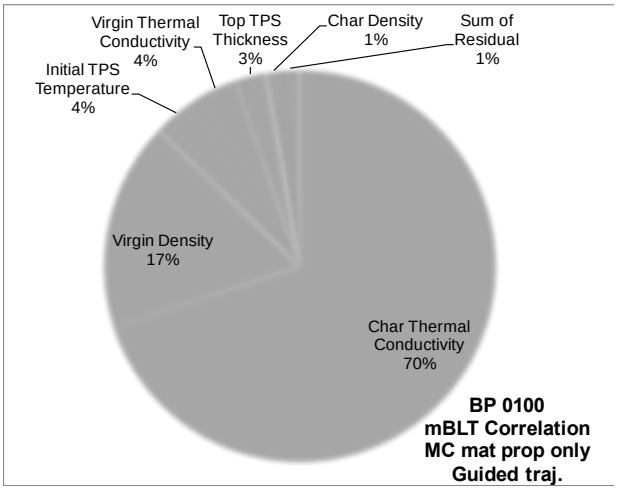

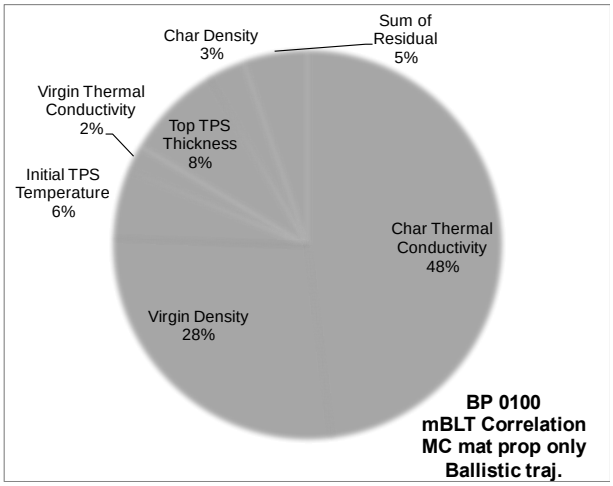

item	CorCoeff	CCsquared
Char Thermal Conductivity	0.836	0.699
Virgin Density	-0.415	0.172
Initial TPS Temperature	0.197	0.039
Virgin Thermal Conductivity	0.191	0.036
Top TPS Thickness	-0.159	0.025
Char Density	0.113	0.013

a) Guided trajectory

item	CorCoeff	CCsquared
Char Thermal Conductivity	0.693	0.480
Virgin Density	-0.525	0.275
Top TPS Thickness	-0.284	0.081
Initial TPS Temperature	0.240	0.057
Char Density	0.177	0.031
Virgin Thermal Conductivity	0.148	0.022

b) Ballistic trajectory

Figure 6. Maximum bond line temperature correlation coefficient values at the stagnation point for the guided and ballistic trajectories

3. Recession correlations

As shown in Fig. 7a, the uncertainty in virgin density has the largest relative correlation (62%) with recession, followed by surface recession rate, B'c (17%), char thermal conductivity (8%) and char density (6%). With a correlation coefficient value of -0.745, virgin density is inversely proportional to recession and is strongly related to it.

For the ballistic trajectory, the relative correlations are shown in Fig 7b. Here, the uncertainty in virgin density has the highest relative correlation at 52%. Next are surface recession rate, B'c (23%) and char thermal conductivity (14%). With a correlation coefficient value of -0.722, virgin density is inversely proportional to recession and is also strongly related to it.

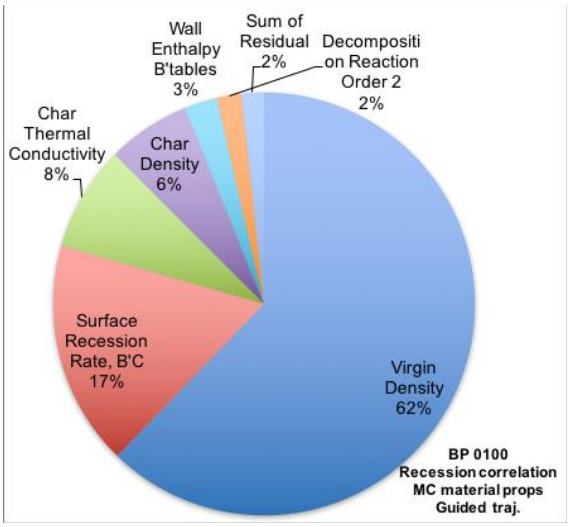

item	CorCoeff	CCsquared
Virgin Density	-0.754	0.568
Surface Recession Rate, B'C	0.396	0.157
Char Thermal Conductivity	-0.271	0.073
Char Density	0.242	0.058
Wall Enthalpy B'tables	-0.152	0.023
Decomposition Reaction Order 2	0.131	0.017

a) Guided trajectory

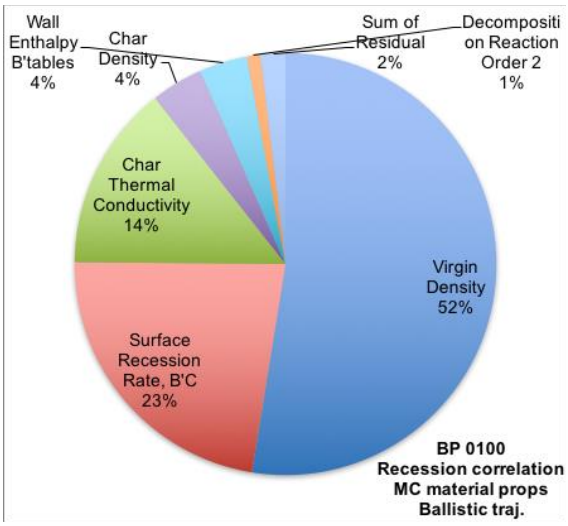

item	CorCoeff	CCsquared
Virgin Density	-0.722	0.521
Surface Recession Rate, B'C	0.473	0.224
Char Thermal Conductivity	-0.376	0.141
Char Density	0.199	0.039
Wall Enthalpy B'tables	-0.191	0.037
Decomposition Reaction Order 2	0.102	0.010

b) Ballistic trajectory

Figure 7. Stagnation point, recession correlation coefficient values

B. Combined results of all body points

This section presents the combined results from all analyzed body points. The analysis results at each individual body point are given in the appendix.

1. Skewness and kurtosis of dispersions (histograms)

Skewness and kurtosis values are indicators of how "Gaussian" is the shape of a dispersion. Skewness and kurtosis values for the mBLT and recession dispersions for all body points and trajectories are given in Table 3. If the dispersion is asymmetrical with respect to the mean value, then the skewness is nonzero and its sign will indicate the direction that the dispersion is skewed. The kurtosis characterizes the sharpness or flatness of the dispersion peak and the wideness or narrowness of the dispersion tails. A kurtosis value greater than 3 indicates[16] a sharper peak and wider tails than for a Gaussian dispersion with the same standard deviation. The only trajectory/body point dispersions with highly non-gaussian skewness and kurtosis occurs for the abort trajectory at body point 2218 (leeside shoulder). These values are misleading, though, because the environment at this body point is so mild that 2% of the cases, (corresponding to low thermal conductivity and high virgin density) have very little rise in mBLT. Neglecting these cases give skewness and kurtosis values well-within Gaussian limits.

Table 3. List of skewness and kurtosis for the mBLT and recession distributions

	guided trajectory				abort trajectory			
	mBLT		recession		mBLT		recession	
Body Point	skewness	kurtosis	skewness	kurtosis	skewness	kurtosis	skewness	kurtosis
0100	0.129	0.018	0.882	0.760	0.268	0.214	0.097	-0.289
0506	0.168	0.088	0.301	0.100	0.132	-0.089	0.154	-0.336
0601	0.223	-0.017	0.030	-0.070	0.291	-0.124	0.068	-0.277
0818	0.155	-0.073	0.002	-0.358	-0.078	2.620	-0.064	1.636
1518	0.148	-0.167	-0.018	-0.272	0.395	-0.268	0.155	-0.496
1617	-0.715	9.525	-0.031	-0.325	0.341	-0.286	0.154	-0.473
2218	0.097	-0.079	0.118	0.045	-5.627	44.042	13.071	549.392

2. 60°C confidence interval at each body point

The confidence interval of 60°C is found using the mBLT dispersion standard deviation (SD) in Eq. 1. The results are summarized in Table 4 and shown at each heat shield location in Fig. 8. These confidence interval results are the principle focus of this work. For the guided trajectory, the lowest confidence interval is 2.56, which is found along the centerline at the windward shoulder acreage. It has body point coordinates of I=06, S=01. For the abort/ballistic trajectory, the lowest confidence interval is 2.16, which occurs at two body point locations (I=16, S=17 and I=22, S=18) at the leeward side, both on and off centerline.

$$60°C\ \text{Confidence Interval} = 60°C/SD(°C) \quad [1]$$

Table 4. Listing of confidence interval by body point and trajectory

BP	SD, °C	60/SD
0100	19.09	3.14
0506	20.07	2.99
0601	23.40	2.56
0818	19.78	3.03
1518	19.48	3.08
1617	20.81	2.88
2218	13.22	4.54

a) Guided trajectory

BP	SD mBLT, °C	60/SD
0100	17.67	3.40
0506	18.61	3.22
0601	22.80	2.63
0818	18.83	3.19
1518	27.30	2.20
1617	27.78	2.16
2218	27.72	2.16

b) Ballistic trajectory

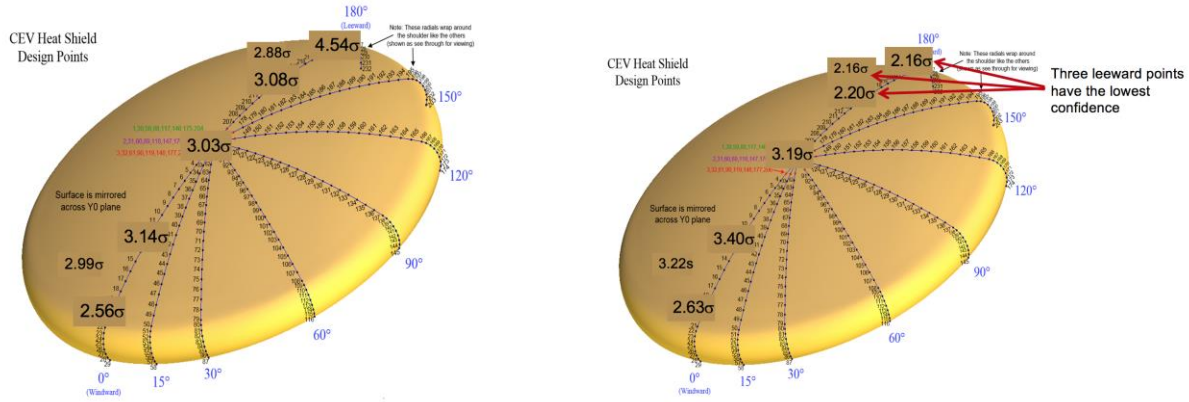

a) Guided trajectory b) Ballistic trajectory

Figure 8. Confidence intervals at heat shield locations for the guided and ballistic trajectories

Shown in Fig. 9 are the relative correlations with mBLT (pie charts) at each body point location for the guided and ballistic trajectories. It is clear that the uncertainty variations in char thermal conductivity and virgin density have the greatest influence in mBLT for every body point considered. For all of the guided trajectory cases, char thermal conductivity has the most relative importance, while this is true for about half of the abort trajectory cases. Recession rate, B'c, and top TPS thickness (due to manufacturing tolerance) are of secondary importance, with top TPS thickness being evident at all body points. Recession rate, B'c is only evident at a few locations.

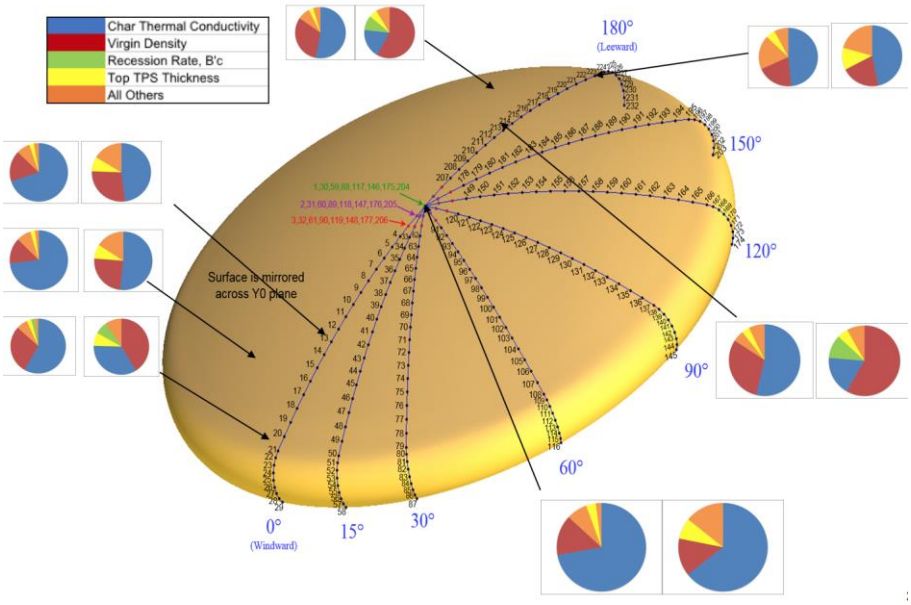

Figure 9. Material property correlations with mBLT. Data pairs are grouped by trajectory: [guided][abort]

Shown in Fig. 10 are the relative correlations with recession (pie charts) at each body point location for the guided and ballistic trajectories. The uncertainty variations in recession rate, B'c, and virgin density have the greatest influence in recession at every body point considered. For all of the guided trajectory cases, char thermal conductivity has the most relative importance, while this is true for about half of the abort trajectory cases. Recession rate, B'c, and top TPS thickness (due to manufacturing tolerance) are of secondary importance, with top TPS thickness being evident at all body points. Recession rate, B'c is only evident at a few locations.

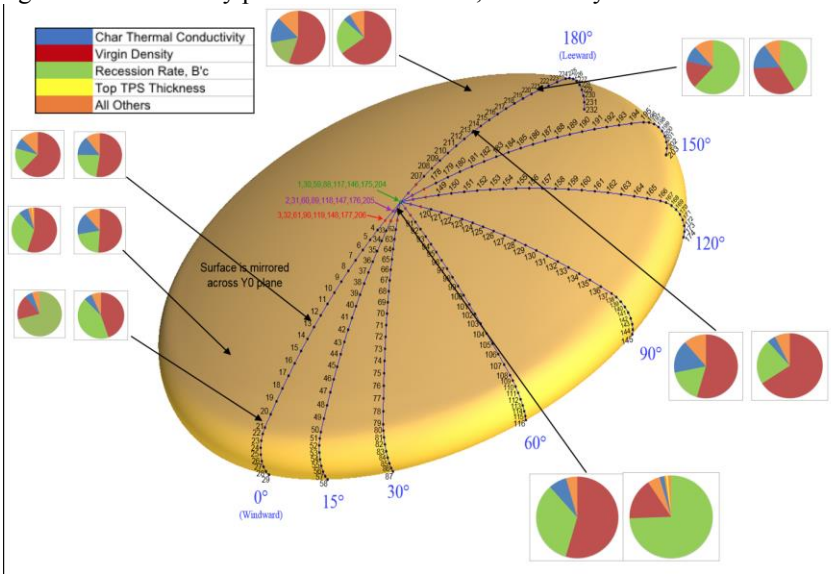

Figure 10. Material property correlations with recession. Data pairs are grouped by trajectory: [guided][abort]

V. Verification

For each monte carlo run, the nominal block Avcoat thickness is found by a CHAR sizing with a maximum allowable bond line temperature of 260°C. The average value of the mcCHAR mBLT dispersion should be close to 260°C, after taking into account the manufacturing tolerance. For the fourteen monte carlo runs (two trajectories and seven body points), these differences are all less than 2°C, indicating very good agreement with between the two.

VI. Conclusions

An investigation of the confidence in the 60°C BTMM has been completed at seven body points using an abort and a guided trajectory. These two trajectories are the driving cases for the current Orion TPS design thickness. For each monte carlo run, ten thousand CHAR runs were completed with a 100% converged solution success rate. For the guided trajectory, the lowest confidence was 2.88, located at the wind side shoulder centerline. For the abort trajectory, the lowest confidence was 2.16, located on the leeward side at both center and off-center locations.

Together, char thermal conductivity and virgin density account for ~ 75% of the relative correlation to mBLT for all body points. Reducing their uncertainty will have the most impact in improving confidence. However, reducing the uncertainty in char thermal conductivity is challenging because its value is very difficult to measure and because a modeler may change its value (within its uncertainty) to better match experimental data. Tuning the value of char thermal conductivity can skew, or even broaden, its uncertainty range.

The material properties with the greatest influence on recession are virgin density, surface recession rate, B'c and char thermal conductivity. Together they account for ~80% of the relative correlation with recession.

The future for mcCHAR and mcFIAT analysis looks encouraging. Their monte carlo routines now include GNC and aerothermodynamics. In addition, Orion flight environments that included gaps and fences on the heat shield surface are also included. The computational goal is to run 20,000 FIAT/CHAR sizings at each of the 321 Orion body points within one day.

Appendix

VII. CHAR Mode and Trajectory Information

Information on the CHAR mode and trajectory is presented in Table 5. The CHAR mode is titled "orion_blocked_avcoat_september_2016." This mode of operation is specific to the Orion program and does not include any heating augmentation due to gaps between Avcoat blocks or "fencing." Fencing is when the height of the adhesive is above that of the ablator due to differential recession rates. This process creates what appears as "fences" between the blocks or tiles. For Orion, fencing is due to the differential recession rates between the EA9394 adhesive and the Avcoat blocks. The trajectory is converted to an aerothermal environment using the perl script evade2char.

Table 5. CHAR code and trajectory information

CHAR version	1.1.0-r5890 (October 7, 2016)
CHAR mode	orion_blocked_avcoat_september_2016
Avcoat model	avcoat_molded_v2.matprops, pge, and bprime
Trajectories	guided: mdac3r5.lun_ei6_nom_fpm5p79_v11p05_m23k_lodp270.fbp.no_unc ballistic/abort: mdac3r5.lun_ei6_cbr_fpm5p79_v11p05_m23k_lodp270.fbp.no_unc • "mdac3r5" is the environment version • "lun" indicates a lunar return mission • "ei6" indicates entry interface case 6, which is the due-north, 3500nmi downrange trajectory • "nom" or "cbr" indicates whether the entry is nominal guided or constant-bank-rate (ballistic) • "fpm5p79" is shorthand for flight path angle = -5.79 deg. • "v11p05" is shorthand for entry velocity = 11.05 km/s • "m23k" is shorthand for CM mass = 23,000 lbm • "lodp270" is shorthand for CM nominal trimmed L/D = 0.27 • "fbp" indicates fixed location body point • "unc or no_unc" indicates whether aerothermal uncertainty factors have been applied to the environment

VIII. Monte Carlo Data Analysis

Presented here is the monte carlo data analysis of the body points that were not presented in the main section of this work.

A. Body point I = 05 S = 06

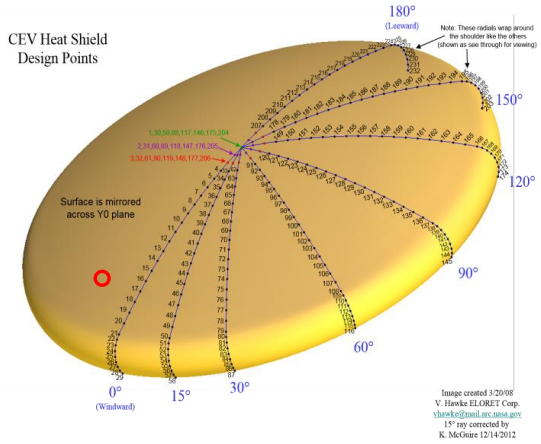

Figure 11. The location of body point I = 05 S = 06 on the heat shield is indicated by the red circle

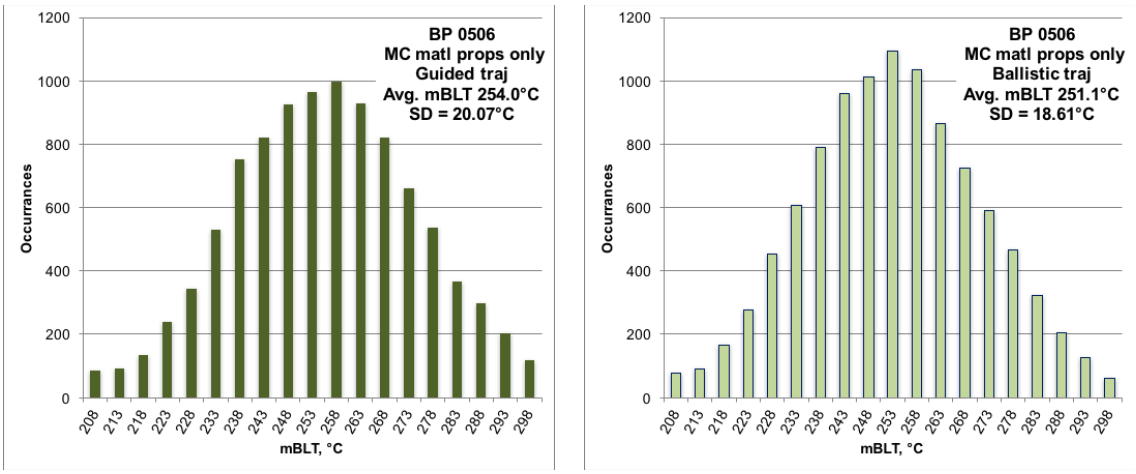

a) b)

Figure 12. Maximum bond line temperature dispersions for the a) guided and b) ballistic trajectories

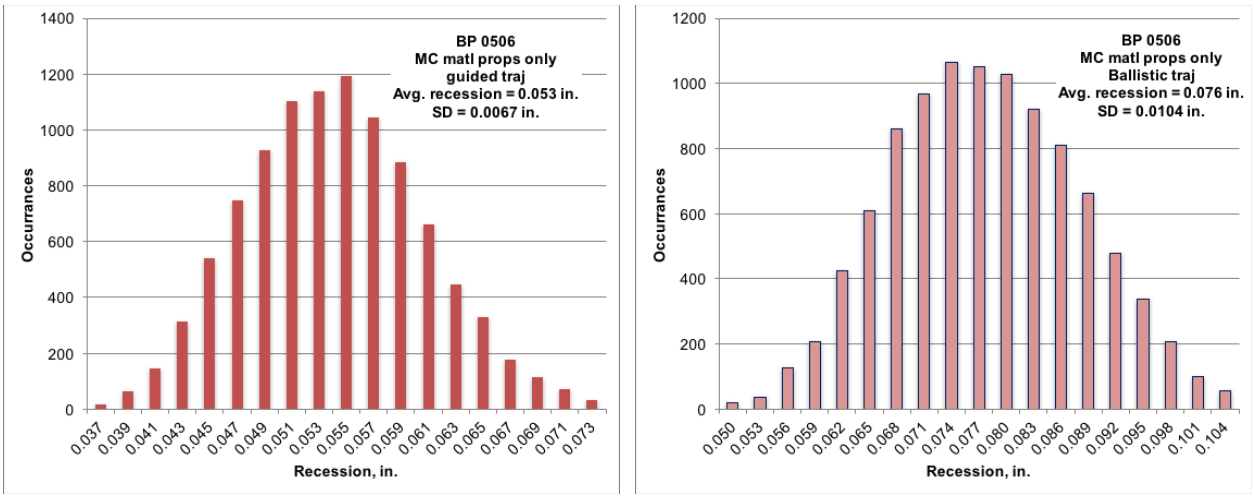

a) b)

Figure 13. Recession dispersions for the a) guided and b) ballistic trajectories

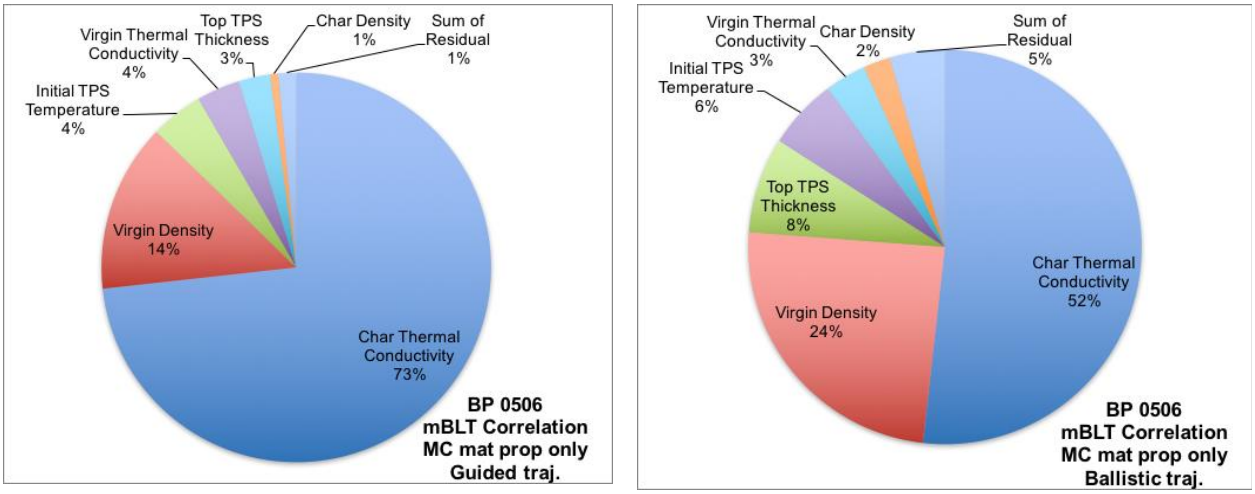

item	CorCoeff	CCsquared
Char Thermal Conductivity	0.853	0.728
Virgin Density	-0.373	0.139
Initial TPS Temperature	0.208	0.043
Virgin Thermal Conductivity	0.189	0.036
Top TPS Thickness	-0.160	0.026
Char Density	0.084	0.007

a)

item	CorCoeff	CCsquared
Char Thermal Conductivity	0.721	0.519
Virgin Density	-0.495	0.245
Top TPS Thickness	-0.280	0.079
Initial TPS Temperature	0.241	0.058
Virgin Thermal Conductivity	0.184	0.034
Char Density	0.149	0.022

b)

Figure 14. Maximum bond line temperature correlations for the a) guided and b) ballistic trajectories

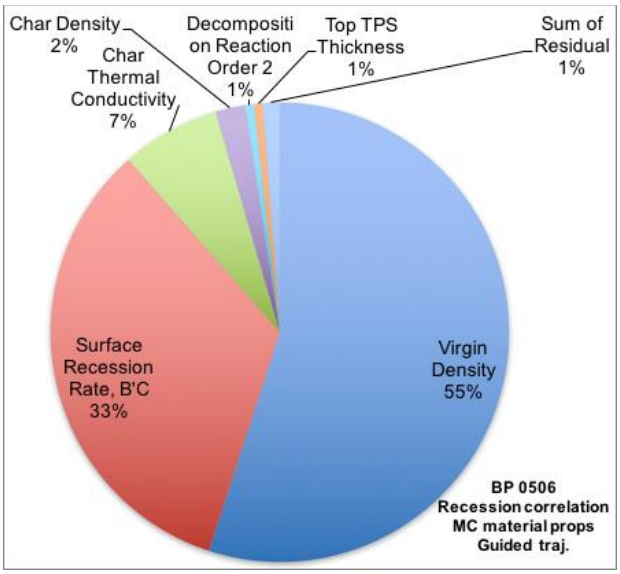

item	CorCoeff	CCsquared
Virgin Density	-0.729	0.531
Surface Recession Rate, B'C	0.569	0.324
Char Thermal Conductivity	-0.259	0.067
Char Density	0.142	0.020
Decomposition Reaction Order 2	0.078	0.006
Top TPS Thickness	-0.076	0.006

a)

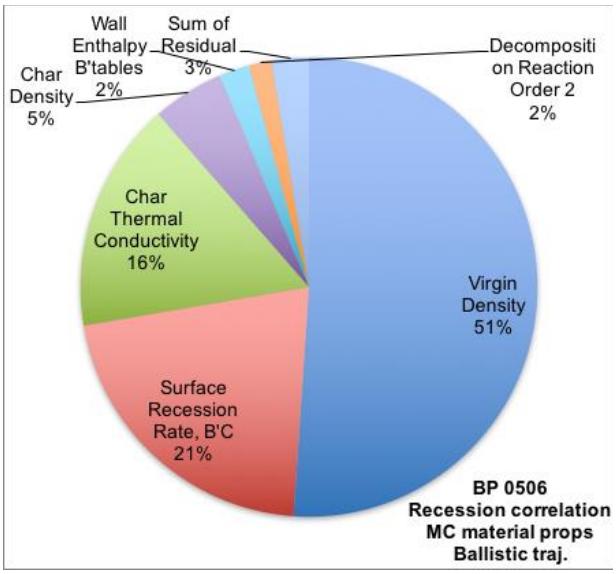

item	CorCoeff	CCsquared
Virgin Density	-0.718	0.516
Surface Recession Rate, B'C	0.463	0.214
Char Thermal Conductivity	-0.405	0.164
Char Density	0.225	0.051
Wall Enthalpy B'tables	-0.148	0.022
Decomposition Reaction Order 2	0.127	0.016

b)

Figure 15. Recession correlations for the a) guided and b) ballistic trajectories

B. Body point I = 06 S = 01

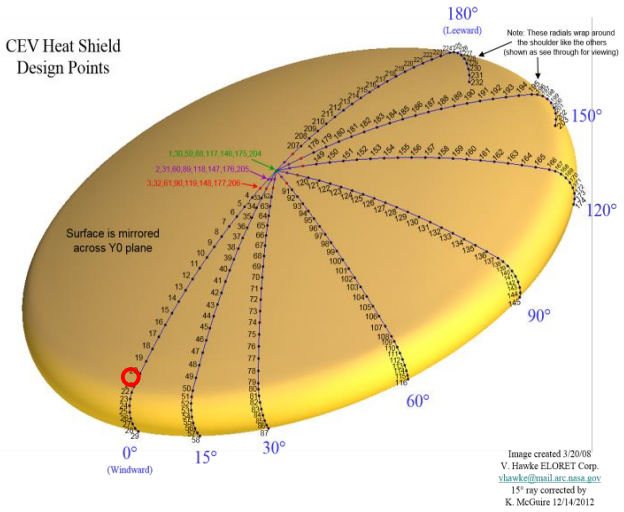

Figure 16. The location of body point I = 06 S = 01 on the heat shield is indicated by the red circle

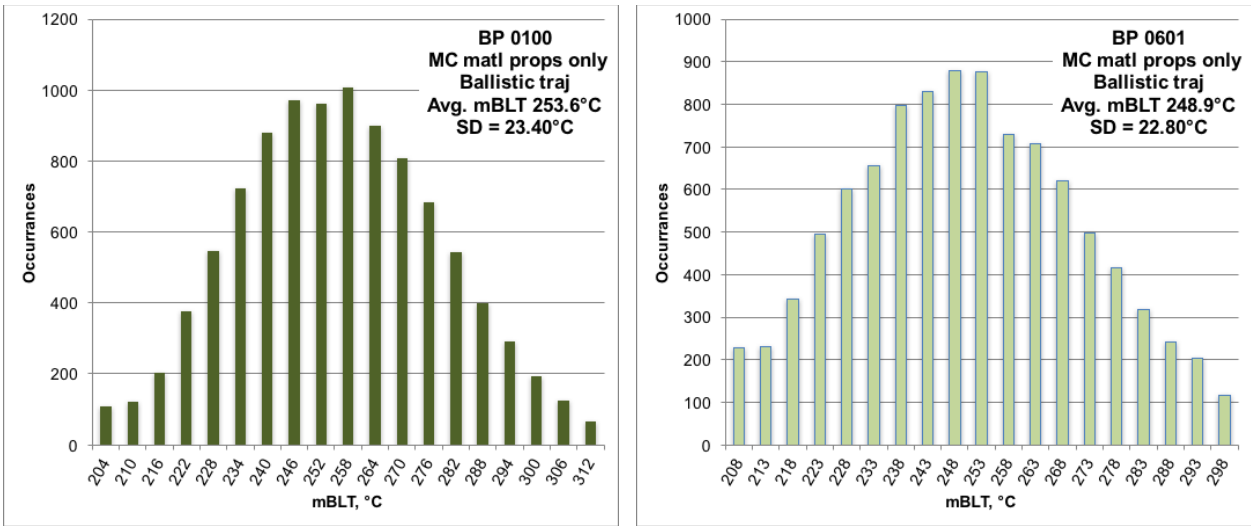

a) b)

Figure 17. Maximum bond line temperature dispersions for the a) guided and b) ballistic trajectories

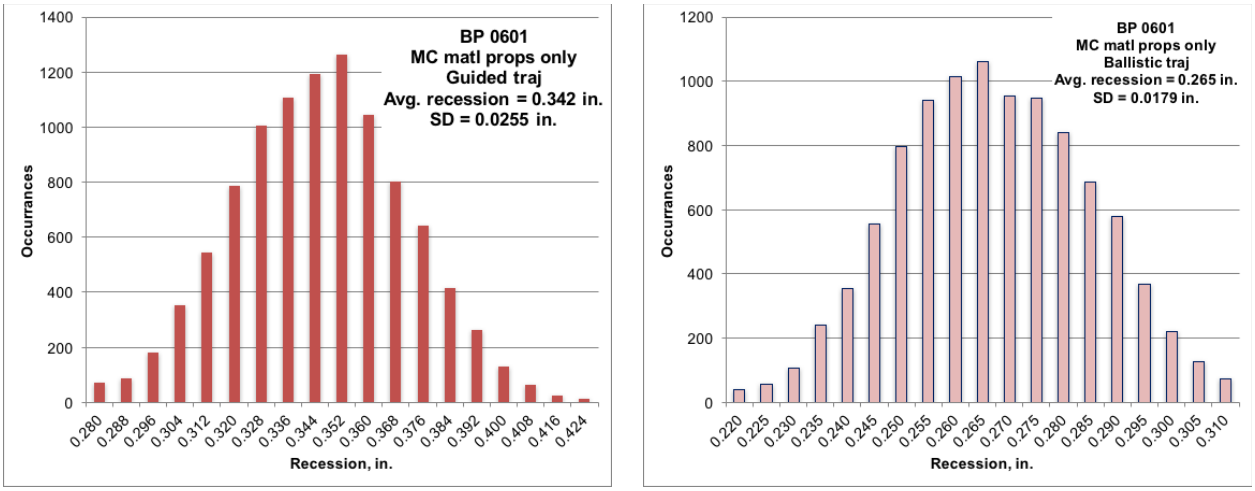

a) b)

Figure 18. Recession dispersions for the a) guided and b) ballistic trajectories

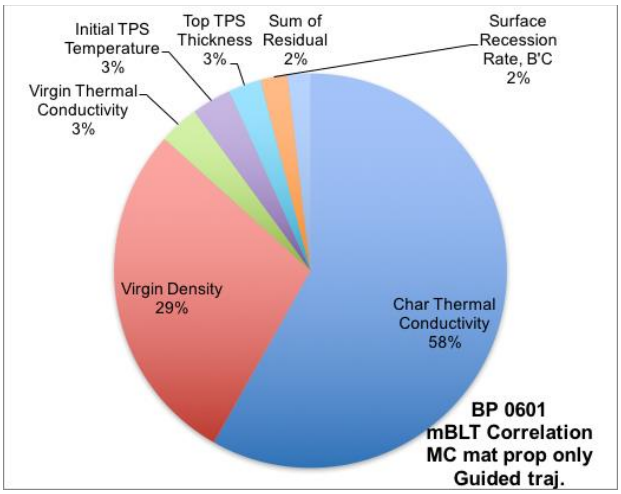

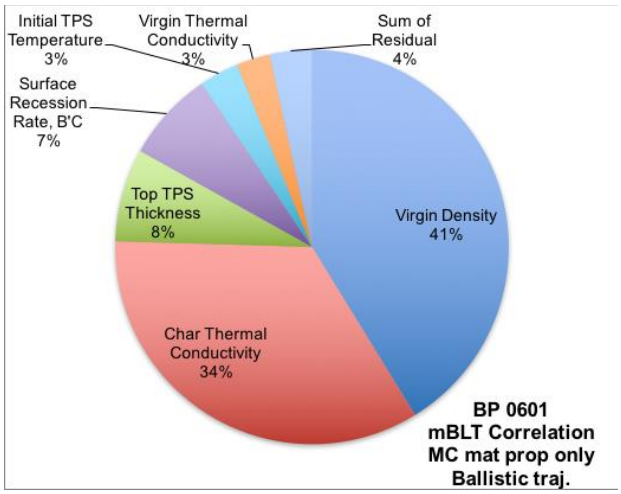

item	CorCoeff	CCsquared
Char Thermal Conductivity	0.764	0.584
Virgin Density	-0.534	0.286
Virgin Thermal Conductivity	0.182	0.033
Initial TPS Temperature	0.181	0.033
Top TPS Thickness	-0.164	0.027
Surface Recession Rate, B'C	0.150	0.022

a)

item	CorCoeff	CCsquared
Virgin Density	-0.642	0.412
Char Thermal Conductivity	0.585	0.342
Top TPS Thickness	-0.276	0.076
Surface Recession Rate, B'C	0.272	0.074
Initial TPS Temperature	0.180	0.032
Virgin Thermal Conductivity	0.166	0.028

b)

Figure 19. Maximum bond line temperature correlations for the a) guided and b) ballistic trajectories

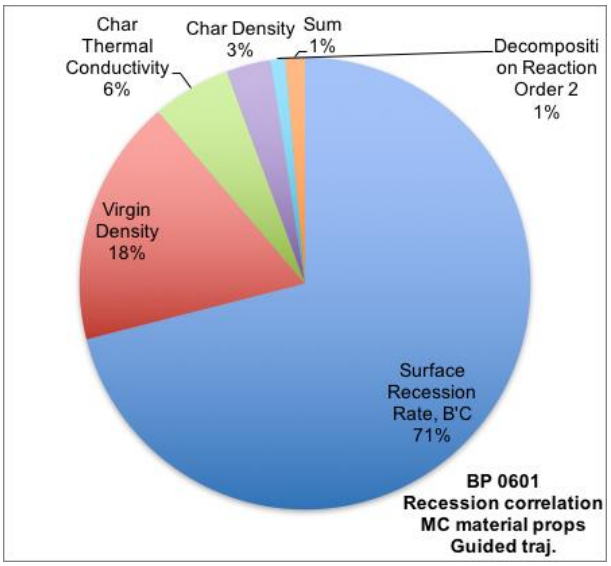

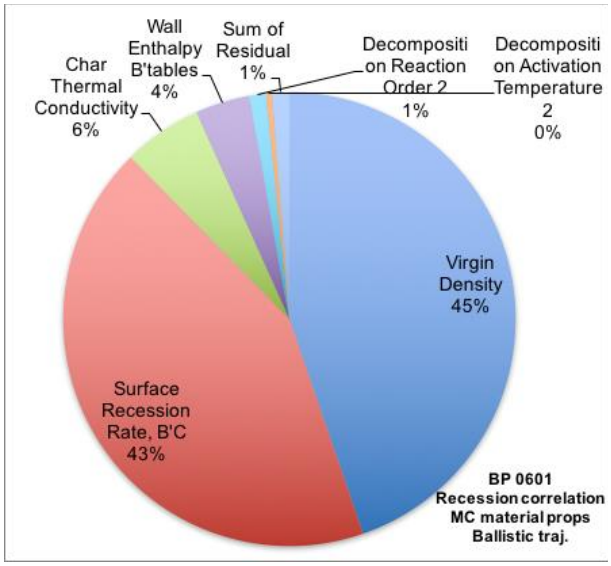

item	CorCoeff	CCsquared
Surface Recession Rate, B'C	0.850	0.723
Virgin Density	-0.424	0.180
Char Thermal Conductivity	-0.240	0.057
Char Density	-0.180	0.032
Decomposition Reaction Order 2	0.104	0.011

a)

item	CorCoeff	CCsquared
Virgin Density	-0.668	0.447
Surface Recession Rate, B'C	0.655	0.429
Char Thermal Conductivity	-0.237	0.056
Wall Enthalpy B'tables	-0.197	0.039
Decomposition Reaction Order 2	0.110	0.012
Decomposition Activation Temperature 2	0.065	0.004

b)

Figure 20. Recession correlations for the a) guided and b) ballistic trajectories

C. Body point I = 15 S = 18

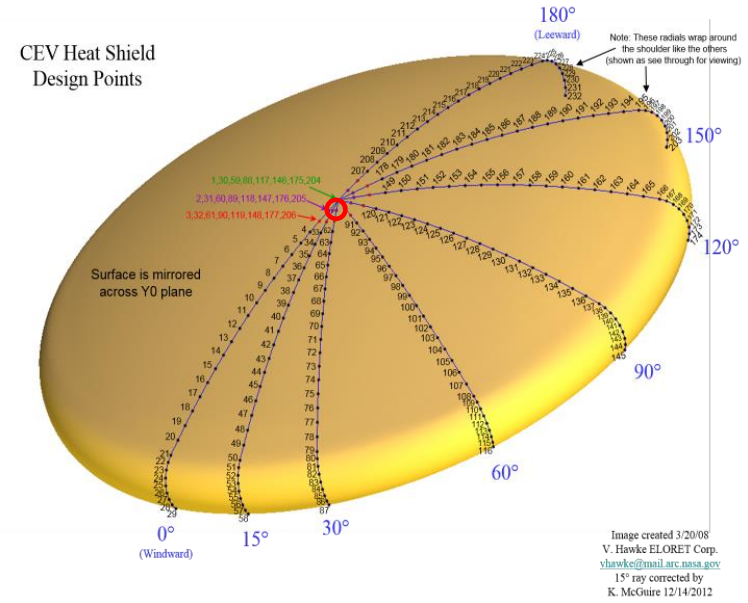

Figure 21. The location of body point I = 15 S = 18 on the heat shield is indicated by the red circle

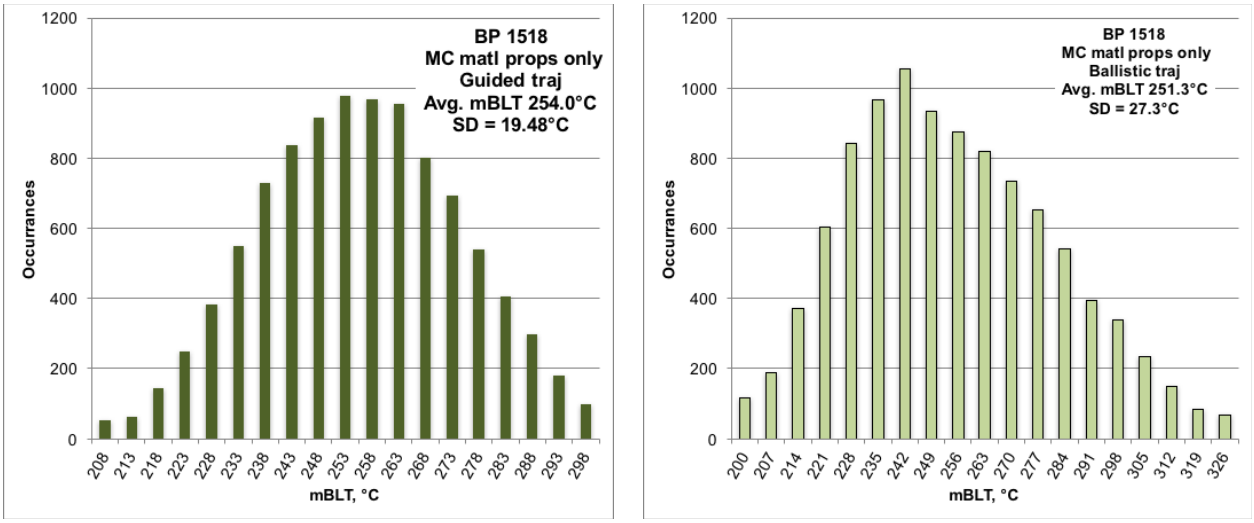

a) b)

Figure 22. Maximum bond line temperature dispersions for the a) guided and b) ballistic trajectories

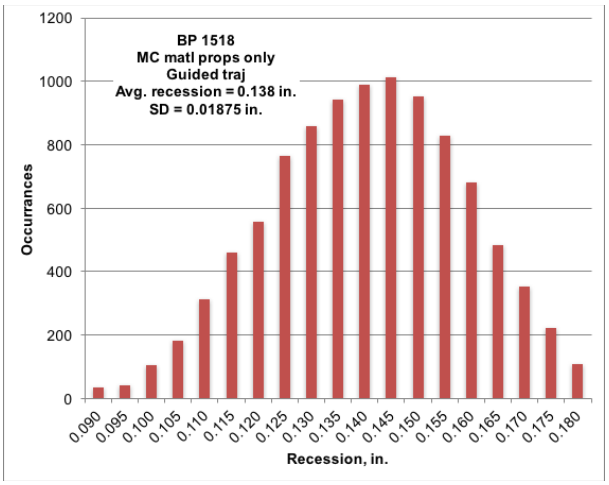

a)

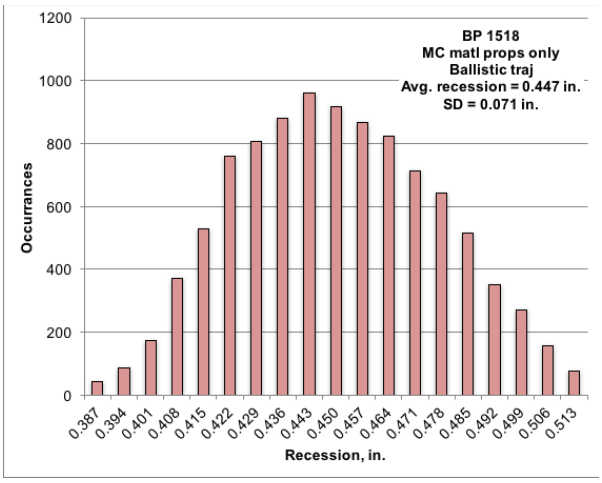

b)

Figure 23. Recession dispersions for the a) guided and b) ballistic trajectories

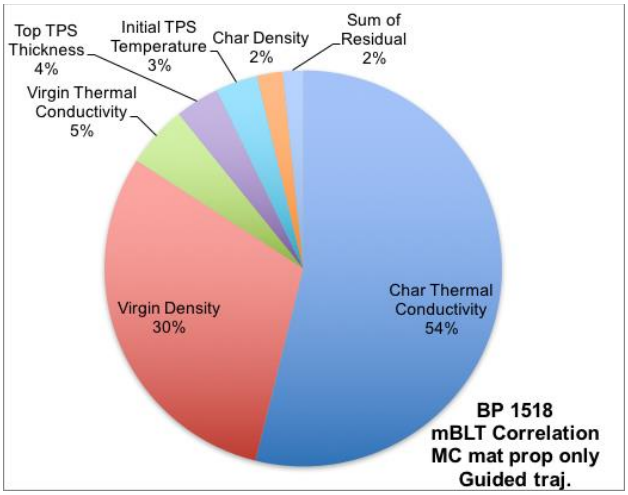

item	CorCoeff	CCsquared
Char Thermal Conductivity	0.729	0.531
Virgin Density	-0.546	0.299
Virgin Thermal Conductivity	0.223	0.050
Top TPS Thickness	-0.188	0.035
Initial TPS Temperature	0.184	0.034
Char Density	0.144	0.021

a)

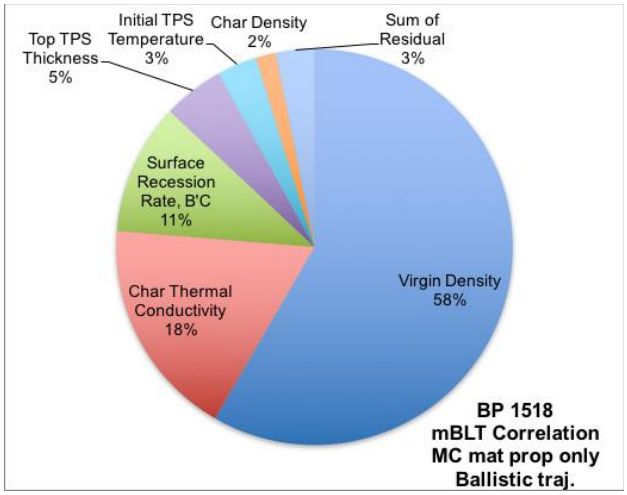

item	CorCoeff	CCsquared
Virgin Density	-0.758	0.575
Char Thermal Conductivity	0.420	0.177
Surface Recession Rate, B'C	0.325	0.106
Top TPS Thickness	-0.221	0.049
Initial TPS Temperature	0.179	0.032
Char Density	0.127	0.016

b)

Figure 24. Maximum bond line temperature correlations for the a) guided and b) ballistic trajectories

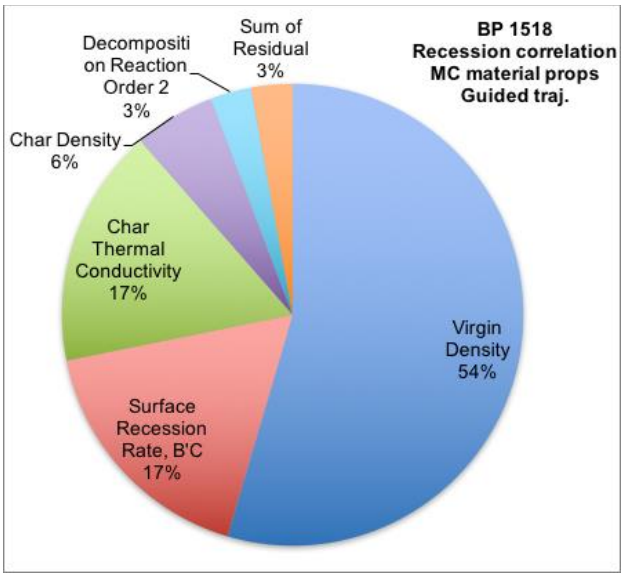

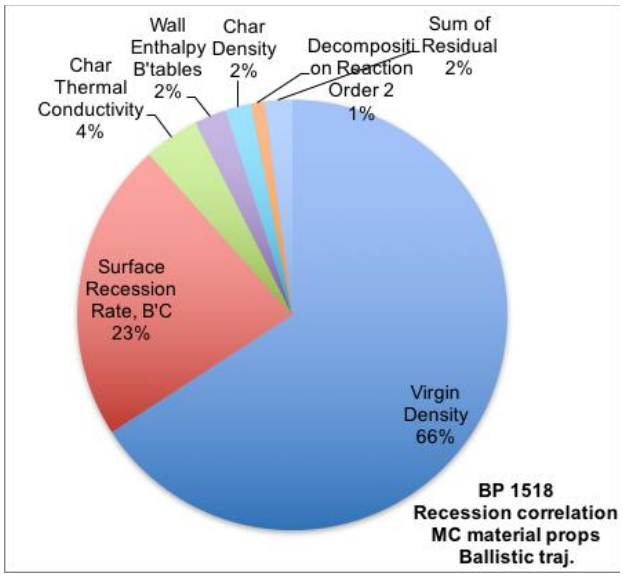

item	CorCoeff	CCsquared
Virgin Density	-0.738	0.545
Surface Recession Rate, B'C	0.415	0.172
Char Thermal Conductivity	-0.409	0.167
Char Density	0.238	0.057
Decomposition Reaction Order 2	0.169	0.029

a)

item	CorCoeff	CCsquared
Virgin Density	-0.809	0.654
Surface Recession Rate, B'C	0.473	0.224
Char Thermal Conductivity	-0.204	0.042
Wall Enthalpy B'tables	-0.153	0.023
Char Density	0.141	0.020
Decomposition Reaction Order 2	0.100	0.010

b)

Figure 25. Recession correlations for the a) guided and b) ballistic trajectories

D. Body point I = 16 S = 17

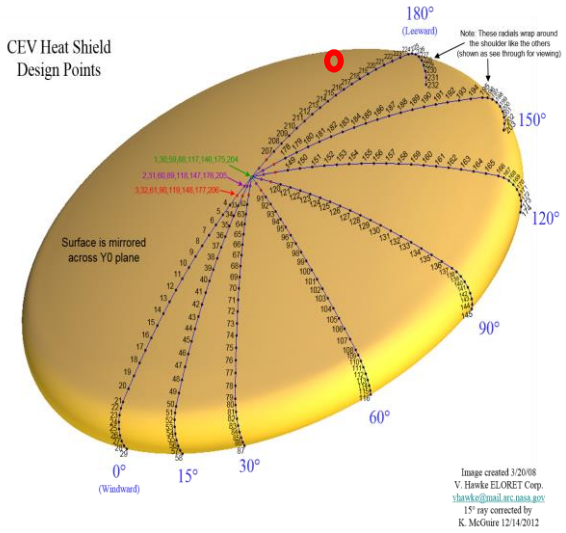

Figure 26. The location of body point I = 16 S = 17 on the heat shield is indicated by the red circle

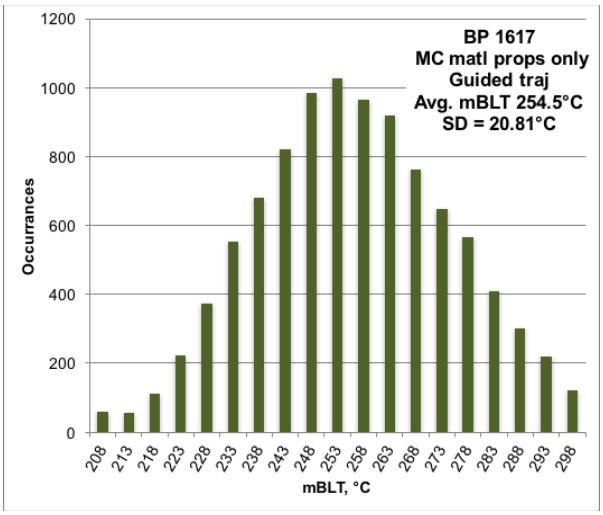

a)

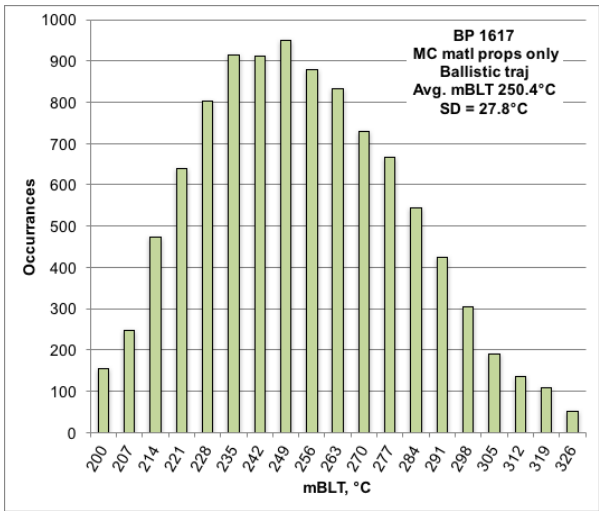

b)

Figure 27. Maximum bond line temperature dispersions for the a) guided and b) ballistic trajectories

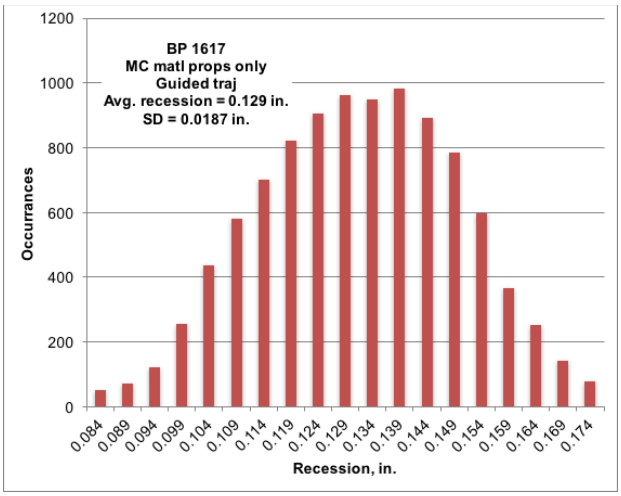

a)

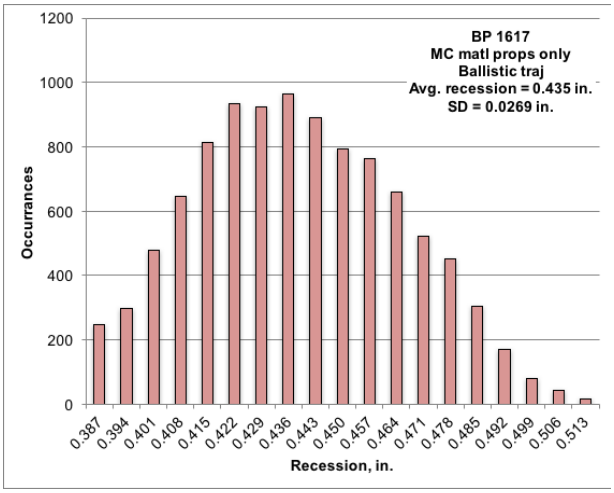

b)

Figure 28. Recession dispersions for the a) guided and b) ballistic trajectories

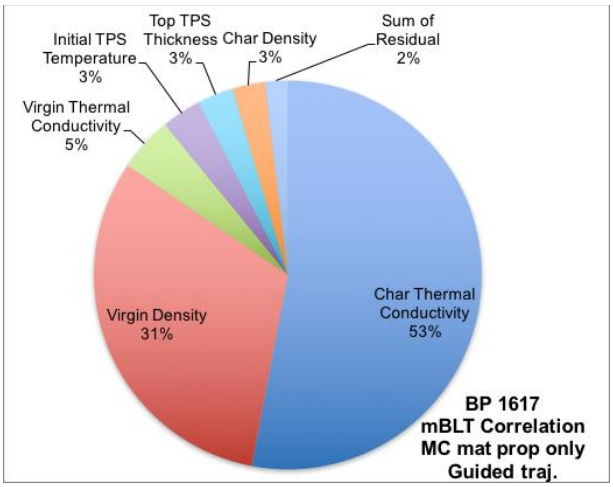

item	CorCoeff	CCsquared
Char Thermal Conductivity	0.696	0.484
Virgin Density	-0.537	0.288
Virgin Thermal Conductivity	0.204	0.042
Initial TPS Temperature	0.174	0.030
Top TPS Thickness	-0.165	0.027
Char Density	0.158	0.025

a)

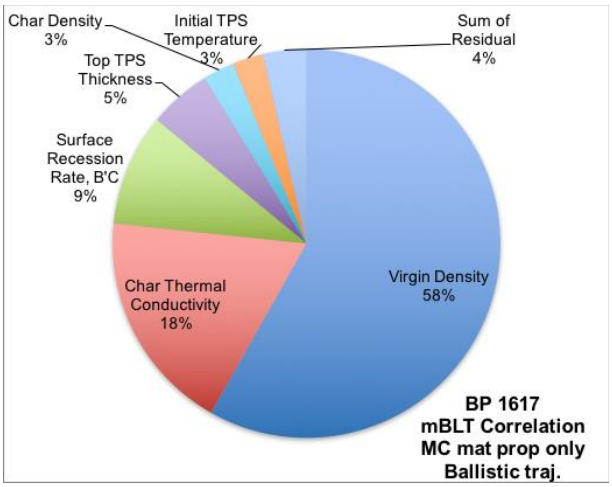

item	CorCoeff	CCsquared
Virgin Density	-0.761	0.579
Char Thermal Conductivity	0.428	0.184
Surface Recession Rate, B'C	0.305	0.093
Top TPS Thickness	-0.228	0.052
Char Density	0.161	0.026
Initial TPS Temperature	0.160	0.026

b)

Figure 29. Maximum bond line temperature correlations for the a) guided and b) ballistic trajectories

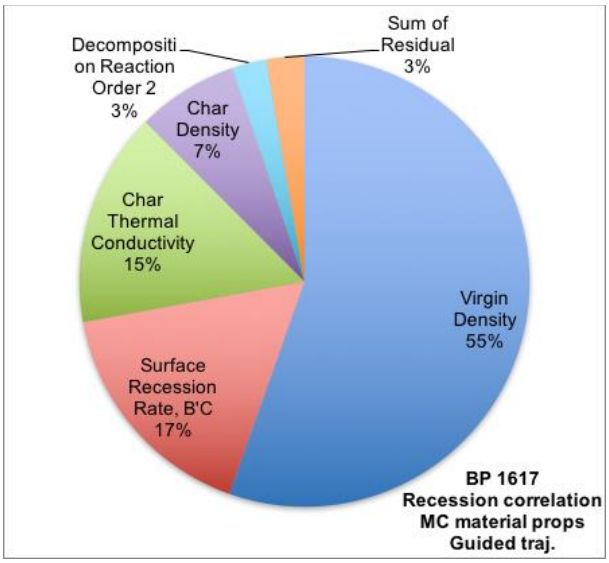

item	CorCoeff	CCsquared
Virgin Density	-0.737	0.544
Surface Recession Rate, B'C	0.405	0.164
Char Thermal Conductivity	-0.389	0.151
Char Density	0.267	0.071
Decomposition Reaction Order 2	0.156	0.024

a)

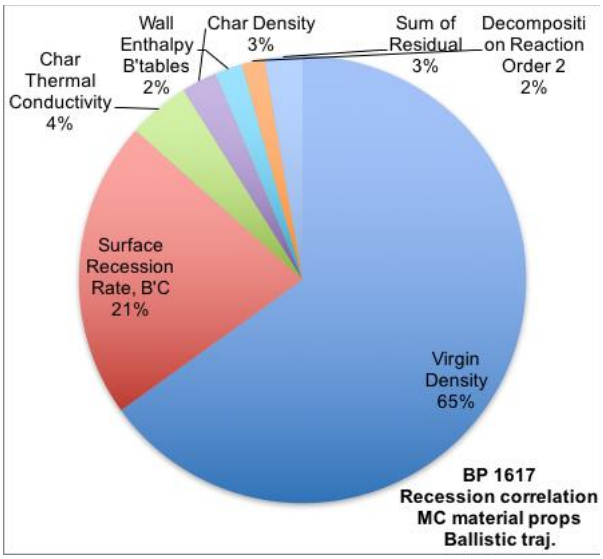

item	CorCoeff	CCsquared
Virgin Density	-0.807	0.651
Surface Recession Rate, B'C	0.465	0.216
Char Thermal Conductivity	-0.212	0.045
Char Density	0.160	0.026
Wall Enthalpy B'tables	-0.141	0.020
Decomposition Reaction Order 2	0.129	0.017

b)

Figure 30. Recession correlations for the a) guided and b) ballistic trajectories

E. Body point I = 22 S = 18

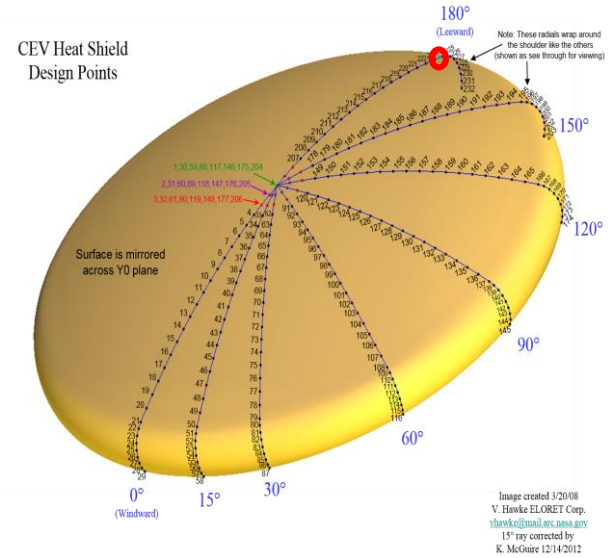

Figure 31. The location of body point I = 22 S = 18 on the heat shield is indicated by the red circle

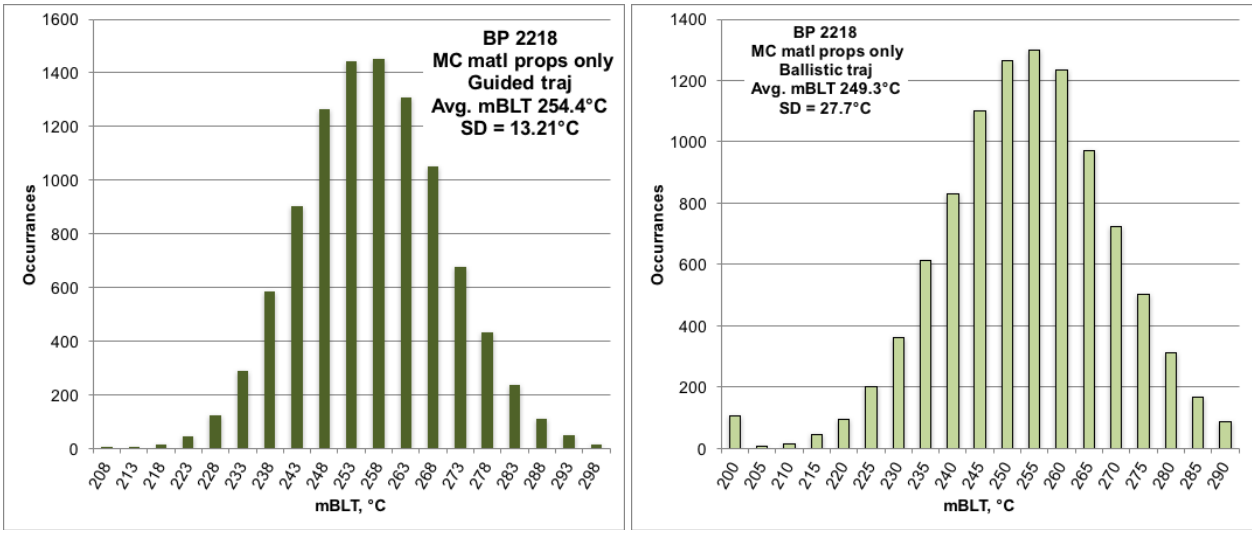

a) b)

Figure 32. Maximum bond line temperature dispersions for the a) guided and b) ballistic trajectories

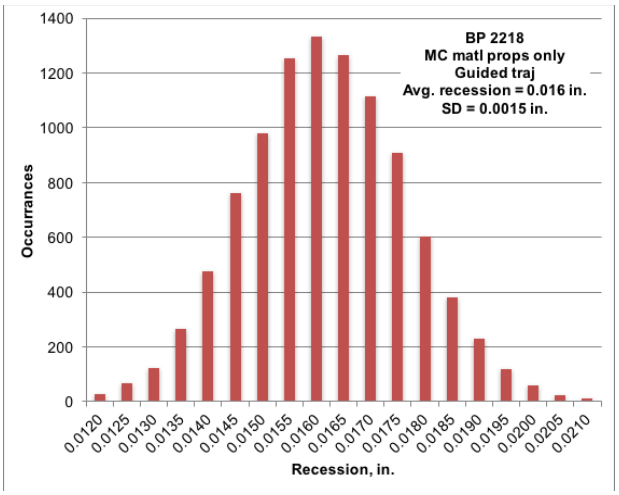

a)

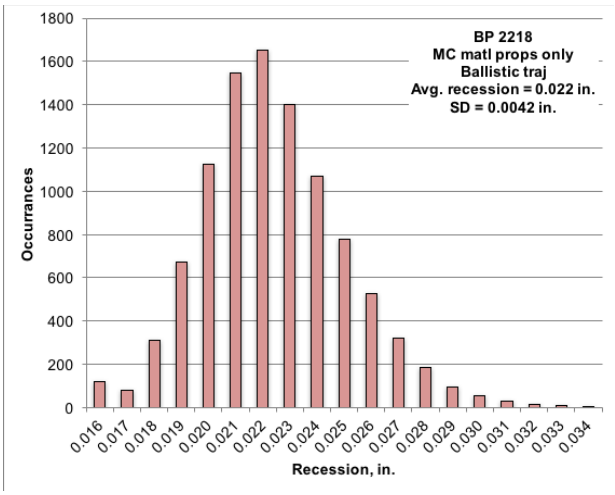

b)

Figure 33. Recession dispersions for the a) guided and b) ballistic trajectories

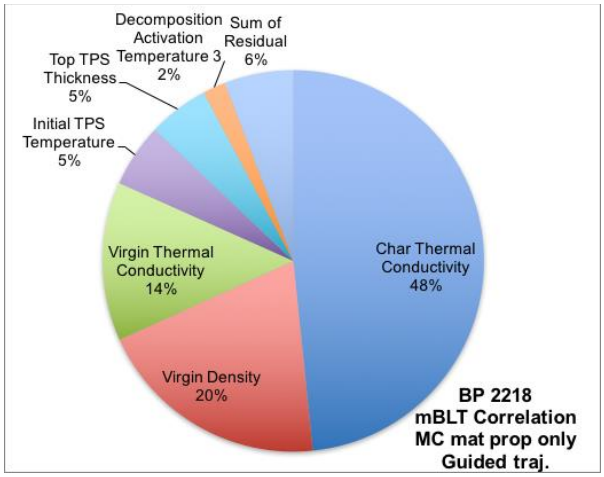

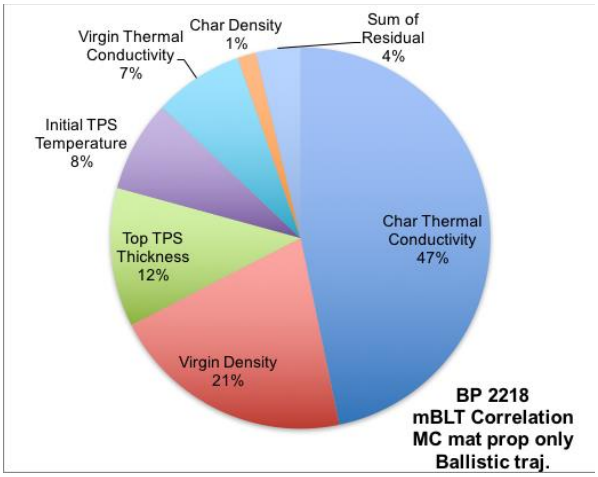

item	CorCoeff	CCsquared
Char Thermal Conductivity	0.685	0.469
Virgin Density	-0.439	0.192
Virgin Thermal Conductivity	0.361	0.131
Initial TPS Temperature	0.228	0.052
Top TPS Thickness	-0.223	0.050
Decomposition Activation Temperature 3	0.137	0.019

a)

item	CorCoeff	CCsquared
Char Thermal Conductivity	0.373	0.139
Virgin Density	-0.248	0.062
Top TPS Thickness	-0.187	0.035
Initial TPS Temperature	0.152	0.023
Virgin Thermal Conductivity	0.151	0.023
Char Density	0.069	0.005

b)

Figure 34. Maximum bond line temperature correlations for the a) guided and b) ballistic trajectories

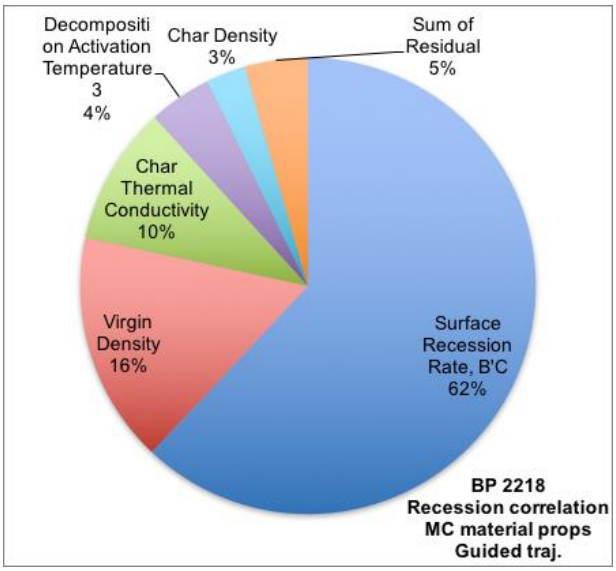

item	CorCoeff	CCsquared
Surface Recession Rate, B'C	0.784	0.615
Virgin Density	-0.403	0.162
Char Thermal Conductivity	-0.312	0.097
Decomposition Activation Temperature 3	0.210	0.044
Char Density	-0.167	0.028

a)

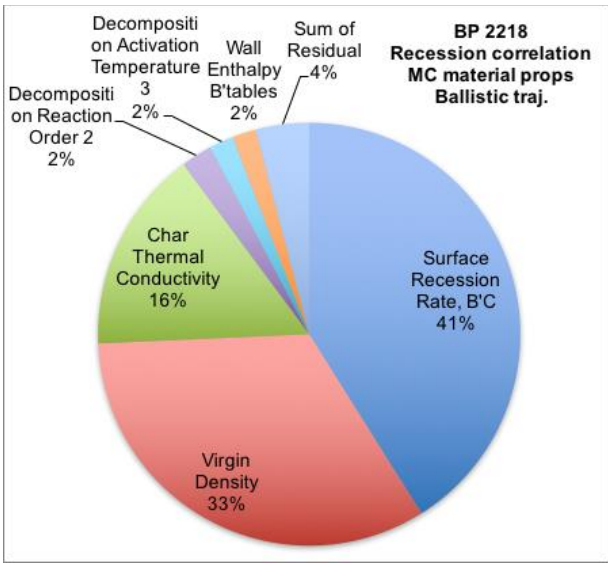

Surface Recession Rate, B'C	0.394	0.155
Virgin Density	-0.354	0.126
Char Thermal Conductivity	-0.242	0.059
Decomposition Reaction Order 2	0.095	0.009
Decomposition Activation Temperature 3	0.084	0.007
Wall Enthalpy B'tables	-0.084	0.007

b)

Figure 35. Recession correlations for the a) guided and b) ballistic trajectories

Acknowledgments

The authors gratefully acknowledge the support provided by the Thermal Protection Materials and Systems Branch of NASA Ames Research Center, through NASA Contract No. NNA 04-BC25C to the AMA Corporation.

References

[1] Chen, Y.-K., and Milos, F. S., "Fully Implicit Ablation and Thermal Analysis Program (FIAT)," Journal of Spacecraft and Rockets,Vol. 36, No. 3, pp 475-483, May–June 1999

[2] Moyer, C. B., and Rindal, R. A., "An Analysis of the Coupled Chemically Reacting Boundary Layer and Charring Ablator – Part II. Finite Difference Solution for the In-Depth Response of Charring Materials Considering Surface Chemical and Energy Balances", NASA CR-1061, 1968.

[3] Amar, A.J., Calvert, N.D., and Kirk, B.S., "Development and Verification of the Charring Ablating Thermal Protection Implicit System Solver" AIAA paper 2011-144, presented at: 49th AIAA Aerospace Sciences Meeting including the New Horizons Forum and Aerospace Exposition, 4 - 7 January 2011, Orlando, Florida

[4] Curry, D. M., "An Analysis of a Charring Ablation Thermal Protection System", NASA TN D-3150, November 1, 1965.

[5] Chen, Y.-K., and Milos, F. S., "Two-Dimensional Implicit Thermal Response and Ablation Program for Charring Materials" J. Spacecraft and Rockets, Vol. 38, No. 4, July– August 2001, pp 473 – 481.

[6] Chen, Y.-K., Milos, F. S., and Gokcen, T., "Validation of a Three-Dimensional Ablation and Thermal Response Simulation Code" AIAA paper 2010-4645, 10th AIAA/ASME Joint Thermophysics and Heat Transfer Conference 28 June - 1 July 2010, Chicago, Illinois

[7] Cozmuta, I., Wright, M.J., Laub. B., and Willcockson, W., "Defining Ablative Thermal Protection System Margins for Planetary Entry Vehicles," AIAA paper 2011-3757, 42nd AIAA Thermophysics Conference AIAA 2011-3757 27 - 30 June 2011, Honolulu, Hawaii

[8] Sepka, S. and Wright, M.J., "Monte Carlo Approach to FIAT Uncertainties with Applications for Mars Science Laboratory" J Thermophysics and Heat Transfer, Vol. 25, No. 4, October–December 2011, pp 516 – 522.

[9] Wright, M.J., Bose, D., and Chen, YK, "Probabilistic Modeling of Aerothermal and Thermal Protection Material Response Uncertainties" AIAA Journal Vol. 45, No. 2, February 2007 pp 399 - 410

[10] Guess, T.R., Reedy, E.D., and Stavig, M.E., "Mechanical Properties of Hysol EA-9394 Structural Adhesive" Sandia National Laboratories, Sandia Report SAND95-0229 UC-704 Unlimited Release Printed February 1995

[11] Kuhbander, R.J., "Characterization Of EA9394 Adhesive For Repair Applications" Interim technical Report for Period September 1, 1988 – April 30, 1992, WL-TR-92-4069, Materials Directorate Wright Laboratory, Air Force Material Command, Wright-Patterson Air Force Base, Ohio 45433- 7734, January 1994

[12] Miki, Mitsunori, Murotsu, Yoshisada, Tanaka, Tetsuo, and Shao, Siaowen, "Reliability Of The Strength Of Unidirectional Fibrous Composites," Amencan Institute of Aeronautics and Astronautics, Inc., 30th Structures, Structural Dynamics and Materials Conference, 1989, paper 1277

[13] Starr, Trevor and Starr, Mary, "Thermoset Resins for Composites: Directory and Databook," Elsever publishing, pp. 126

[14] Sater, Janet M., Rigdon, Michael A., "Graphite-Reinforced Polycyanate Composites for Space And Missile Applications," Institute For Defense Analyses, prepared For Ballistic Missile Defense Organization, IDA Document D-1454, November, 1993, pp 3-13 and D-119

[15] Coughlin, S., William, S., Sepka, S., McGuire, M., "Determination of Uncertainties for Analytically Derived Material Properties to be used in Monte Carlo Based Orion Heatshield Sizing" AIAA paper to be presented at AIAA Scitech 2018, Kissimmee, FL.

[16] Steinwolf, A., Rizzi, S., "Non-Gaussian Analysis of Turbulent Boundary Layer Fluctuating Pressure on Aircraft Skin Panels" JOURNAL OF AIRCRAFT Vol. 43, No. 6, November–December 2006, pp 1662 - 1675